

Numerical simulation of hydraulic fracturing using a three-dimensional fracture model coupled with an adaptive mesh fluid model

Guo, L., Xiang, J. and Latham, J.-P.

Department of Earth Science and Engineering, Imperial College London, South Kensington Campus, London SW7 2AZ, United Kingdom

Viré, A.

Faculty of Aerospace Engineering, Delft University of Technology, 2629HS Delft, The Netherlands

Pavlidis, D. and Pain, C. C.

Department of Earth Science and Engineering, Imperial College London, South Kensington Campus, London SW7 2AZ, United Kingdom

Copyright 2015 ARMA, American Rock Mechanics Association

This paper was prepared for presentation at the 49th US Rock Mechanics / Geomechanics Symposium held in San Francisco, CA, USA, 28 June-1 July 2015.

This paper was selected for presentation at the symposium by an ARMA Technical Program Committee based on a technical and critical review of the paper by a minimum of two technical reviewers. The material, as presented, does not necessarily reflect any position of ARMA, its officers, or members. Electronic reproduction, distribution, or storage of any part of this paper for commercial purposes without the written consent of ARMA is prohibited. Permission to reproduce in print is restricted to an abstract of not more than 200 words; illustrations may not be copied. The abstract must contain conspicuous acknowledgement of where and by whom the paper was presented.

ABSTRACT: A three-dimensional fracture model developed in the context of the combined finite-discrete element method is incorporated into a two-way fluid-solid coupling model. The fracture model is capable of simulating the whole fracturing process. It includes pre-peak hardening deformation, post-peak strain softening, transition from continuum to discontinuum, and the explicit interaction between discrete fracture surfaces, for both tensile and shear fracture initiation and propagation. The fluid-solid coupling model can simulate the interactions between moving fluids and multi-body solids. By incorporating the fracture model into the coupling model, a methodology of using the new coupling model to capture fracturing behaviour of solids in fluid-solid coupling simulations is proposed. To solve the problem in the coupling model of having adaptive continuous meshes being used by the fluid code and discontinuous meshes in the solid code, a scheme to convert different meshes is developed. A single fracture propagation driven by fluid pressures is simulated and the results show that the modelling obtains the correct critical load and propagation direction for fluid-driven fracturing. Several important phenomena, such as stress concentration ahead of the fracture tip, adaptive refinement of fluid mesh as a response to the fracture propagation and fluids flowing into fractures, are properly captured.

1. INTRODUCTION

Hydraulic fracturing has been used in the oil and gas industry for more than half a century. It is particularly important for the extraction from unconventional reservoirs, which otherwise would be considered as uneconomical. In the research field of hydraulic fracturing, an increasing amount of effort has been put into the development of novel numerical models to simulate realistic scenarios. However, the numerical modelling of hydraulic fractures still remains a challenge for computational mechanics because of the complexities in fluid-solid coupling, fracture characterisation, and particularly in three dimensions, the complicated geometry and topology update when fractures propagate. In recently years, many attempts have been made and significant progress achieved in three-dimensional hydraulic fracturing simulations.

Carter et al. (2000) [1] proposed a fully three-dimensional hydraulic fracture model, but they neglected the fluid continuity equation in the area around the fracture. Secchi and Schrefler (2012) [2] developed a method to simulate three-dimensional hydraulic fractures in porous media and presented an example of a concrete dam. In this paper, a three-dimensional fracture model is incorporated into a two-way fluid-solid coupling model for hydraulic fracture simulations. The three-dimensional fracture model is capable of simulating the whole fracturing process. It includes pre-peak hardening deformation, post-peak strain softening, transition from continuum to discontinuum, and the explicit interaction between discrete fracture surfaces, for both tensile and shear fracture initiation and propagation. After incorporating it into the fluid-solid coupling model, where the interaction between fluids and solids can be explicitly simulated, the initiation and

propagation of fractures can be driven by forces generated both from solids loading and transferred from fluids loading, e.g. fluid pressure, which significantly extends the application of this fracture model into some very important areas that would not be possible with only solids modelling, e.g. the simulation of hydraulic fractures.

The focus of this paper is to introduce the new three-dimensional coupling model with the fracture model and present a numerical example of modelling fluid-driven fractures. This paper is organised as follows. First, the three-dimensional fracture model and the original two-way fluid-solid coupling model are briefly introduced. Second, the overall methodology of the new coupling model with fracture model is proposed and the special difficulties in computational implementation are addressed. Last, a numerical example of modelling fluid-driven fractures is presented.

2. 3D FRACTURE MODEL

The three-dimensional fracture model used in this paper was developed in the context of the combined finite-discrete element method (FEMDEM) [3] in the first author's PhD project [4]. In the FEMDEM simulations, the entire domain is treated as a multi-body system and each discrete element is further discretised into a mesh of finite elements. The finite element formulation is used to simulate continuum behaviour for each discrete body, which includes the calculation of strain and stress in finite elements. The discrete element formulation is used to simulate discontinuum behaviour, e.g. contact interaction between discrete bodies and across discontinuities, which means the calculation of contact force and the distribution of contact force to finite element nodes. The fracture model links the finite element formulation with the discrete element formulation. For each intact discrete body, before fracture initiation, the stresses are calculated by the finite element formulation; if the stress state meets the failure criterion, a discrete fracture will form and then the interaction between discrete fracture surfaces will be modelled explicitly by the contact algorithms in the discrete element formulation; therefore, the whole process of transition from continuum to discontinuum can be realistically and accurately captured.

In the fracture model, a three-dimensional domain is discretised by 4-node tetrahedral elements and 6-node joint elements, which are inserted between tetrahedral elements. A mesh of two tetrahedral elements is taken as an example to illustrate the procedure of space discretisation in Fig. 1. Fig. 1a shows two adjacent tetrahedral elements 1 and 2 sharing three nodes a , b and c in a continuous mesh. Then these two tetrahedra are detached (Fig. 1b), so they do not share nodes any more, which means all three nodes a , b and c are being

duplicated; new nodes a_1 , b_1 and c_1 belong to tetrahedral element 1, and a_2 , b_2 and c_2 belong to tetrahedral element 2. It should be noted that at this initial pre-processing stage, there is no deformation caused by any form of loading in the domain, so every pair of nodes a_1 - a_2 , b_1 - b_2 and c_1 - c_2 have the same coordinates but different node numbers in the mesh topology. The gap between tetrahedral elements 1 and 2 in Fig. 1b is exaggerated only for illustration purpose to show that they do not share any nodes. Last the duplicated nodes a_1 , b_1 , c_1 , c_2 , b_2 and a_2 are renumbered as $N_1 \sim N_6$, respectively, and a 6-node joint element $N_1N_2N_3-N_4N_5N_6$ is inserted between tetrahedral elements 1 and 2 (Fig. 1c), whose continuity is therefore constrained by the joint element.

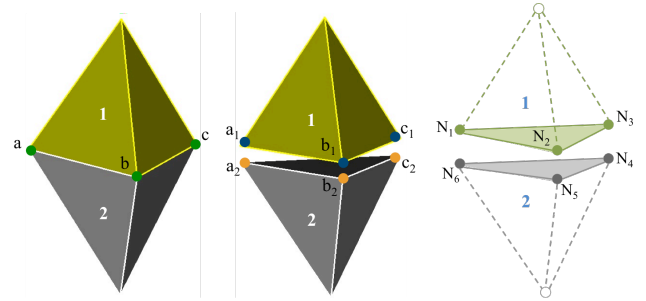


Fig. 1. Schematic illustration of inserting a joint element between two tetrahedral elements.

The normal stress and shear stress in joint elements are calculated by the relative distances between tetrahedral elements, and follow a stress-displacement relation, which includes a strain softening part after the peak stress [5]. The softening material behaviour represents the plastic zone ahead of a real fracture. A Mohr-Coulomb failure criterion with a tension cut-off is used to determine the failure states of joint elements. The shear strength is dependent on the normal stress acting perpendicular to the shear direction. Therefore, fracturing behaviour both in tensile and shear modes can be simulated in complex stress fields. The failure of joint elements would physically separate tetrahedral elements and generate discrete fractures. The details of this fracture model can be found in [4,6].

3. FLUID-SOLID COUPLING MODEL

The three-dimensional two-way fluid-solid coupling model is developed on the basis of the FEM-based fluid code Fluidity-ICOM and the FEMDEM-based solid code Y3D. The fluid code Fluidity-ICOM is a finite element open-source numerical code that solves non-hydrostatic Navier-Stokes equations on unstructured meshes. The coupling model belongs to the category of loosely coupled modelling, which means the fluid and solid dynamics equations are solved in separate numerical models and information is exchanged between the two models. In the coupling model, the solids are fully immersed in the fluids, so it is a type of immersed body method.

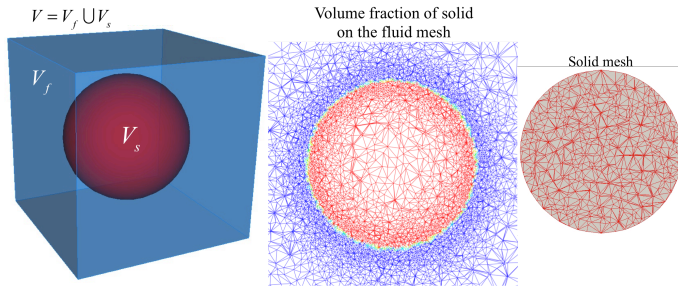


Fig. 2. An example of a fluid-solid coupling domain. (a) a solid domain V_s (red colour) immersed in a fluid domain V_f (blue colour), so the whole domain $V = V_f \cup V_s$; (b) a cross-section of the fluid mesh, where the solid domain is represented by a volume fraction on the fluid mesh (red colour); (c) a cross-section of the solid mesh.

An example of a solid sphere immersed in fluids is shown in Fig. 2 to illustrate the basic concepts of the original fluid-solid coupling model. In this example, the solid domain V_s (sphere) is fully immersed in the fluid domain V_f (

Fig. 2a). The subscripts s and f are used to denote the solids and the fluids, respectively. The interaction between solids and fluids is simulated by filling the volumes covered by solids with the surrounding fluids and relaxing the flow to the solid behaviour in these volumes. The whole domain V , $V = V_f \cup V_s$, is discretised by the so-called fluid mesh (

Fig. 2b), which is the mesh used in the fluid code of the coupling model; meanwhile, an independent solid mesh (Fig. 2c) is only used to discretise the solid domain V_s , which is the mesh used in the solid code of the coupling model. It should be noted that in the fluid model, the solid domain is also discretised and represented by a volume fraction on the fluid mesh, while in the solid model, it only discretises the solid domain and the fluid domain is not included. It should also be noted that the solid mesh (used by the solid code) is fixed, which means it does not change during the simulation, while the fluid mesh (used by the fluid code) can be dynamically updated to increase accuracy and reduce computational cost at the same time. In the current coupling model, the fluids are assumed to be incompressible, and therefore the solids that are compressible are modelled through time variations of a volume fraction in the fluid domain. In this way, incompressible and compressible materials are modelled in a compatible mass conserving way. Details of the above-mentioned coupling model can be found in [7,8].

4. NEW FLUID-SOLID COUPLING MODEL WITH FRACTURE MODEL

4.1. Overall scheme

The fluid-solid coupling model was originally developed for simulating the interactions between moving fluids and multi-body solids, with an assumption that the solids

cannot break. In the applications like hydraulic fracturing, however, fluids play a dominant role in the fracture propagation. Therefore, fracturing of solids must be taken into account in these kinds of coupling simulations. The flowchart of the new fluid-solid coupling model with the fracture model is shown in Fig. 3.

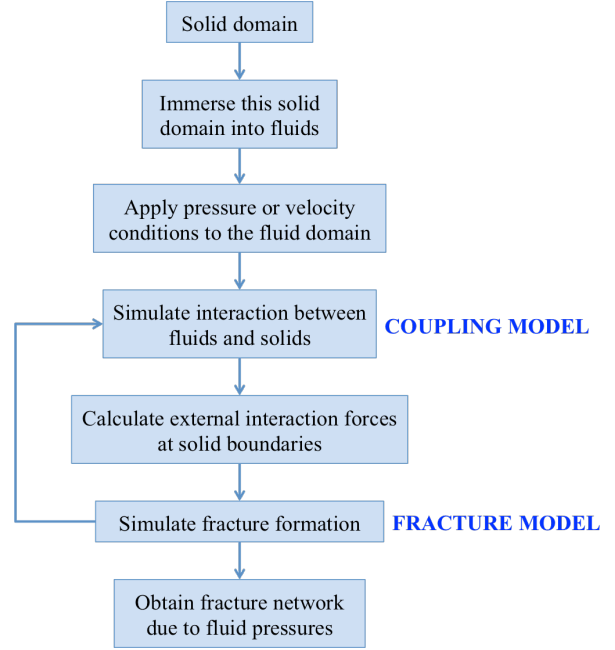


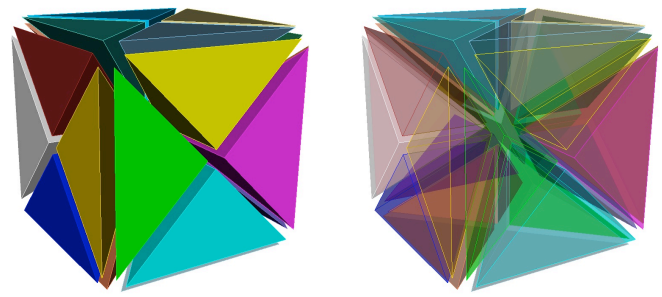
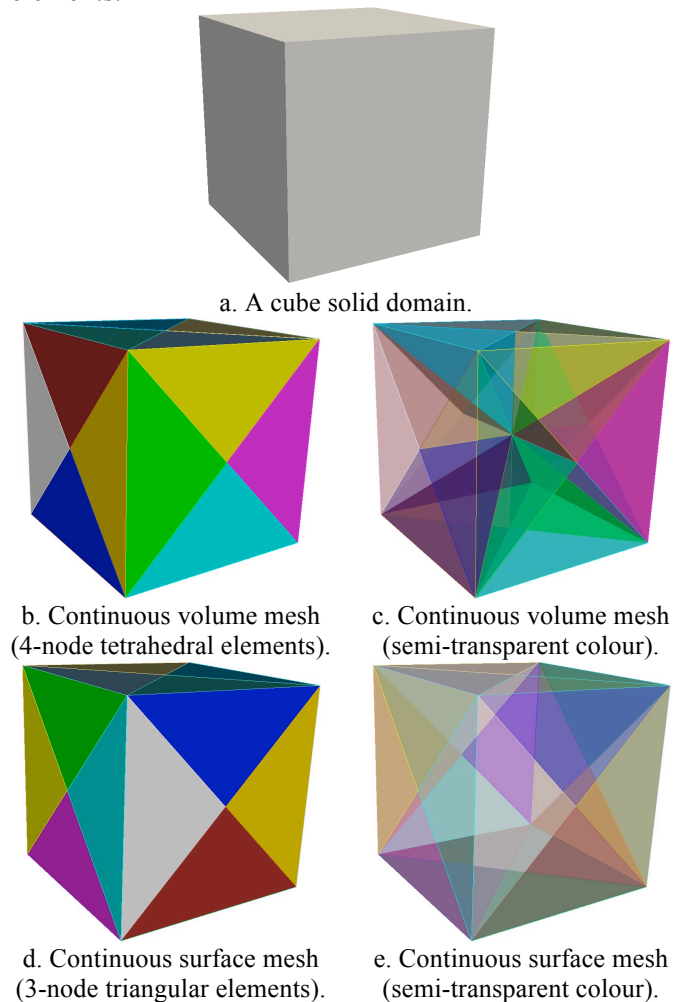
Fig. 3. Flowchart of fracture modelling in the coupling simulations.

4.2. Computational implementation

In order to incorporate the three-dimensional fracture model into the fluid-solid coupling model, there are several difficulties to overcome in the computational implementation. A fundamental incompatibility between the coupling model and the fracture model is the difference in meshes. The fluid mesh used by the coupling model is continuous, which consists of two parts: a continuous volume mesh of 4-node tetrahedral elements and a continuous surface mesh of 3-node triangular elements. The surface mesh covers the solid domain, which characterises the interface between fluids and solids. By contrast, the solid mesh used by the fracture model is discontinuous, which is a mixed volume mesh of 4-node tetrahedral elements and 6-node joint elements. Here the terms ‘continuous’ and ‘discontinuous’ are used to describe the continuity between adjacent elements. In the continuous volume mesh, adjacent tetrahedral elements share nodes; so do the adjacent triangular elements in the continuous surface mesh. In the discontinuous volume mesh, however, adjacent tetrahedral elements do not share nodes, and they are connected by joint elements.

The difference between meshes is illustrated by an example of a cube solid domain shown in Fig. 4. The geometry of this cube domain is shown in Fig. 4a. In

Fig. 4b, this cube domain is discretised by a continuous volume mesh of 4-node tetrahedral elements, where faces, edges and nodes of tetrahedral elements are shared by adjacent elements. Note that a semi-transparent colour scheme is used to show the inside of the domain in Fig. 4c and the mesh is the same as in Fig. 4b. In Fig. 4d and e, only the boundary surfaces of this cube domain are discretised by a continuous surface mesh of 3-node triangular elements. Similarly to the continuous volume mesh, in this continuous surface mesh, edges and nodes of triangular elements are shared by adjacent elements. In Fig. 4f and g, the same cube domain is discretised by a discontinuous volume mesh of 4-node tetrahedral elements and 6-node joint elements. It should be noted that in these two figures the gaps between tetrahedral elements are exaggerated to represent the existence of joint elements. In this mesh, tetrahedral elements are separated by joint elements so it is called a discontinuous volume mesh. Each face, edge and node exclusively belongs to one tetrahedral element, i.e. no adjacent tetrahedral elements share faces, edges or nodes. The continuity of tetrahedral elements is not enforced by geometric connectivity but by the joint elements.



f. Discontinuous volume mesh (4-node tetrahedral elements and 6-node joint elements).

g. Discontinuous volume mesh (semi-transparent colour).

Fig. 4. A cube solid domain represented by different meshes. A semi-transparent colour scheme is used in figures (c), (e) and (g) to show the inside of the domain. Note that in figures (f) and (g) the gaps between tetrahedral elements are exaggerated to represent the existence of joint elements.

The different meshes used by the fluid code and the fracture model in the solid code creates an incompatibility problem because the coupling model needs to project variables on element nodes between the fluid mesh and the solid mesh but this projection cannot be conducted directly between a continuous mesh and a discontinuous mesh. To guarantee force balance is achieved on a certain fracture surface represented by a projection of the fluid mesh onto the broken joint elements, the discontinuous mesh used by the fracture model is converted into a continuous mesh, which is also dynamically updated with the fracture propagation. It should be noted that the converted continuous mesh, including a continuous volume mesh and a continuous surface mesh, is only used by the fluid code, while for the solid code with the fracture model, the mesh is still discontinuous. Details of this mesh converting and updating scheme can be found in the first author's PhD thesis [4].

5. NUMERICAL EXAMPLE

5.1. Model setup

The numerical example presented here is a simulation of a single fracture propagation driven by fluid pressures. The model setup is shown in Fig. 5. The dimensions of the solid domain are $100 \text{ mm} \times 49 \text{ mm} \times 50 \text{ mm}$, which are the height, width and thickness in the y , x and z -direction, respectively. A pre-existing wedge-shaped fracture is inserted at the middle of the model and extends uniformly through the model in the z -direction. The largest opening of this fracture is at the left-hand boundary, which is 2.45 mm , and then linearly decreases to zero at the fracture tip, which spreads 24.5 mm from the left-hand boundary into the model in the x -direction. Therefore, the aspect ratio of this wedge-shaped pre-

existing fracture, which is defined by opening/length, equals 1/10. The fluid domain surrounds the solid domain and is not explicitly shown in Fig. 5. The solid material represents a typical competent limestone rock and the fluids are of high viscosity, which is necessary to guarantee numerical stability using the current version of the coupling code.

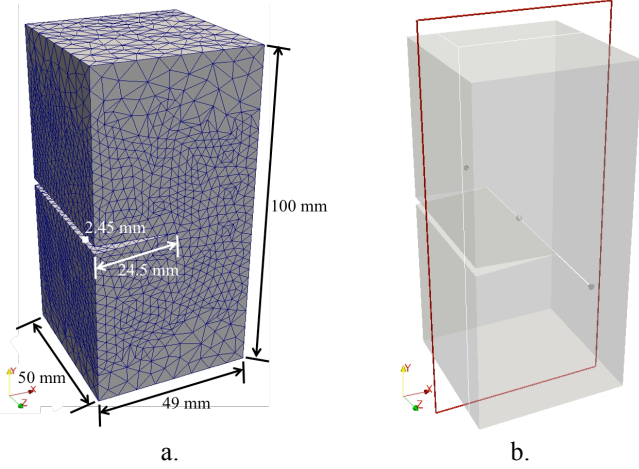


Fig. 5. Model setup for the simulation of a single fracture propagation driven by fluid pressures. (a) dimensions and mesh of the model; (b) a cut plane perpendicular to the z -direction and passing through the centre of the model, which is used to show two-dimensional contours in the result section.

It can be seen from Fig. 6a that the fluid domain surrounds the solid domain, which corresponds to the concept of ‘immersed body’ used for fluid-solid coupling. The loading condition for the fluid domain is a pressure condition P , which is first allowed to equilibrate at 15 MPa and then increases from 15 MPa at a loading rate of 2×10^4 MPa/s. Under this loading rate it takes less than one millisecond for the fracture to propagate through the domain (see the results in Section 5.2). The solid domain is stressed by a polyaxial pressure boundary condition, which represents *in situ* stresses. Three pressures 20 MPa, 15 MPa and 10 MPa are applied to the boundary surfaces of the solid domain (Fig. 6b). It should be noted that here the engineering mechanics sign convention is employed, which means tensile stress is positive and compressive stress is negative. Therefore, under this convention in Fig. 6b, the maximum principal stress $\sigma_1 = -10$ MPa ($\sigma_2 = -15$ MPa, $\sigma_3 = -20$ MPa, $\sigma_1 > \sigma_2 > \sigma_3$) is applied in the vertical y -direction. However, if the geomechanics sign convention is used, where compressive stress is positive and tensile stress is negative, the stress in the vertical y -direction should be the minimum principal stress $\sigma_3 = 10$ MPa ($\sigma_1 = 20$ MPa, $\sigma_2 = 15$ MPa, $\sigma_1 > \sigma_2 > \sigma_3$). The initial fluid pressure of 15 MPa and *in situ* stresses are designed to generate an initial tensile stress of 5 MPa in the vertical y -direction, which equals the tensile strength f_t of the solid material (e.g. a typical limestone [9]).

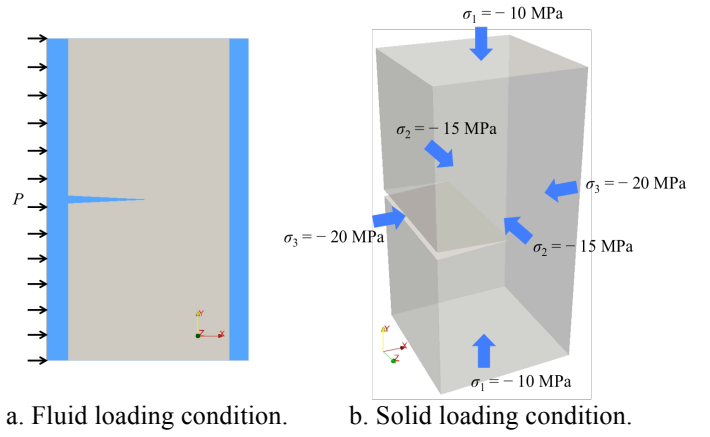


Fig. 6. Fluid and solid loading conditions in the simulation. (a) The solid domain (grey colour) is surrounded by fluids (blue colour), and the loading for the fluid domain is a pressure condition P . (b) The loading condition for the solid domain is a polyaxial pressure boundary condition, where three different pressures are applied to the boundary surfaces perpendicular to the three orthogonal directions x , y and z , respectively. Note that the engineering mechanics sign convention is used here, which means tensile stress is positive and compressive stress is negative.

In this example, the time-step used in the fluid code $\Delta t_f = 2.5 \times 10^{-6}$ s and the time-step used in the solid code $\Delta t_s = 5 \times 10^{-9}$ s, so the solid code runs 500 time-steps per fluid time-step. This is because the fluid code employs an implicit time integration scheme while the solid code uses explicit time integration. In order to resolve the stress wave propagation in the solid domain, and because stress waves normally propagate much faster in solids, the solid time-step is much smaller than the fluid time-step, which unavoidably causes the problem of time staggering between solid and fluid models because their equations are not solved simultaneously. However, the small time-steps used in the fluid code, which means the time-steps used in the solid code are even smaller, ensure that the time-conservation error arising from the time staggering problem does not affect the accuracy of the results [7]. An unstructured mesh is used for the solid domain. The average tetrahedral element size is ~ 5 mm at the upper and lower boundaries and gradually reduces to ~ 2 mm near the pre-existing fracture. It should be noted that the solid mesh is fixed so does not change during the simulation, while the fluid mesh can be dynamically updated, e.g. adaptively refining near fluid-solid interfaces according to change in volume fraction of solid and coarsening elsewhere.

5.2. Numerical results

The numerical results are shown in Fig. 7. Driven by fluid pressures, the single fracture propagates nearly horizontally until reaching the right-hand boundary of the solid domain. The irregular fracture path is attributed to the mesh dependency because the fracture can only propagate along tetrahedral element boundaries. The

stress component shown in Fig. 7 is the vertical stress in the y -direction, which is parallel to the general normal direction of the fracture surface so governs the propagation of this mode I type fracture. From the vertical stress contours, it can be seen that the stress concentration ahead of the actual fracture tip is correctly captured by the fracture model in the solid code of the coupling model.

The fracture propagation can also be seen from the solid concentration contours, which is defined to distinguish the fluid domain and the solid domain, where the value of 1 means pure solids (red area) and 0 means pure fluids (blue area). It can be seen that although the opening of the newly developed fracture is very small, some fluids have already flowed into it. The fluid mesh used by the fluid code in the coupling model is very refined near fluid-solid interfaces and relatively coarse elsewhere, and is adaptively updated with the fracture propagation, which continuously generate new fluid-solid interfaces. As the new fracture surfaces define new fluid-solid interfaces, the fracture propagation can also be viewed as the spread of the refinement in the fluid mesh. It should be noted that in Fig. 7c and d, the fracture patterns seen from the solid code output, i.e. the three-dimensional fracture patterns, the two-dimensional patterns and the vertical stress contours, are different from the fluid code output, i.e. the solid concentration contours and the adaptive meshes. Basically, the fracture propagation seen in the fluid code is slightly behind the actual fracture propagation in the solid code, which is caused by the continuous mesh updating algorithm. When joint elements fail, they will definitely generate discrete fractures in the discontinuous mesh used in the solid code. However, when the discontinuous mesh is converted into a continuous mesh for the fluid code in the coupling model, only the failed joint elements that satisfy certain conditions are taken into account to split the continuous mesh and generate discrete fracture surfaces. Therefore, those failed joint elements that do not satisfy these conditions are neglected at the current time-step, and will only be processed after some time-steps when they satisfy the conditions. As a suggestion for future improvement, a solution to this lagging problem is proposed in the first author's PhD thesis [4].

6. DISCUSSION

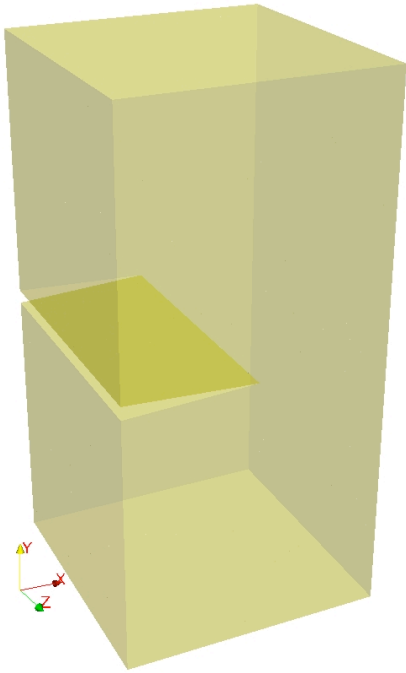
The fluid-solid coupling model with the fracture model correctly captures a single fracture propagation driven by fluid pressures. The main components of the modelling of hydraulic fracturing are addressed in the numerical example presented in this paper. However, it should be noted that one key part is neglected in the current coupling model, which is the poro-elastic fluid exchange between matrix rock and the fracture fluid, sometimes

referred to as fluid leak-off [10-12]. Another limitation of the current coupling model is that the incompressible fluid assumption may be leading to greater numerical instability. To solve the above-mentioned issues, research has been in progress to extend the coupling model to compressible fluids, where the fracture model can be exploited in the future for more applications, e.g. blasting fragmentation simulations.

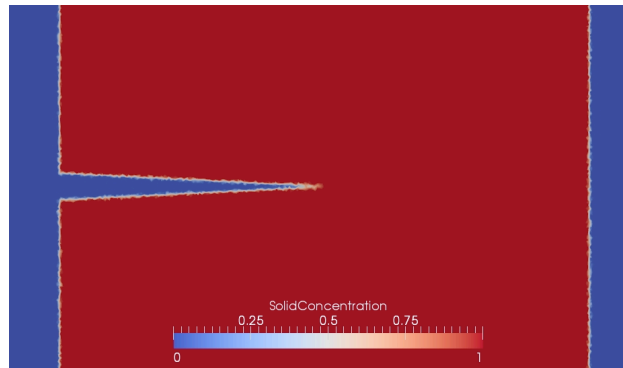
7. CONCLUSIONS

The three-dimensional fracture model was incorporated into a two-way fluid-solid coupling model. A methodology of using this model to capture hydraulic fracturing behaviour in fluid-solid coupling simulations was proposed. To solve the problem that different meshes are used by the fluid code and the solid code in the coupling model, a scheme to convert the discontinuous volume mesh used by the solid code with the fracture model into a continuous volume mesh and a continuous surface mesh used by the fluid code was developed. A numerical example of a fluid-driven fracture simulation was presented and the results were analysed from both the fluid code and the solid code output.

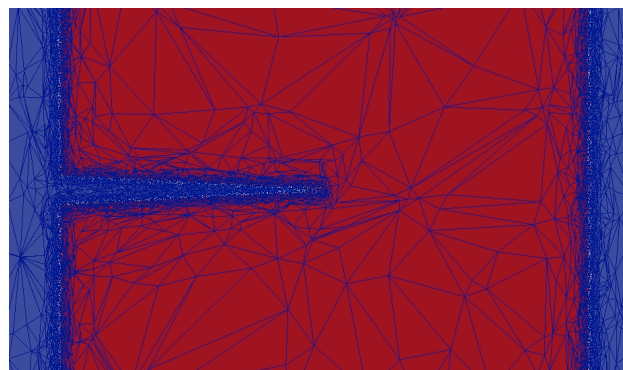
The new fluid-solid coupling model with the fracture model is capable of simulating fractures in coupling simulations. One major application of this model is the simulation of hydraulic fracturing, e.g. fluid-driven fractures, where fluid pressures play a dominant role in the fracture propagation. The numerical example presented in this paper shows that the coupling model with the fracture model obtains the correct critical load and propagation direction for fluid-driven fractures. Several important phenomena, such as stress concentration ahead of the fracture tip, adaptive refinement of fluid mesh as a response to the fracture propagation and fluids flowing into fractures, are properly captured in the numerical test. It is worth mentioning that more quantitative benchmark tests, e.g. based on internally pressurised boreholes, and more complicated simulations, e.g. the interaction between hydraulic fractures and natural fractures, need to be done to validate this model and broaden its application area.



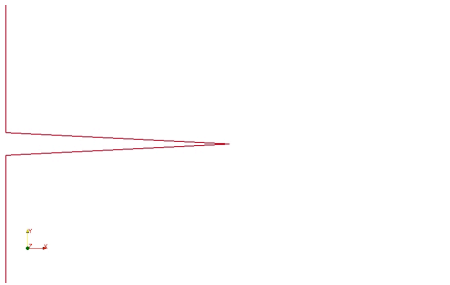
Three-dimensional fracture pattern.



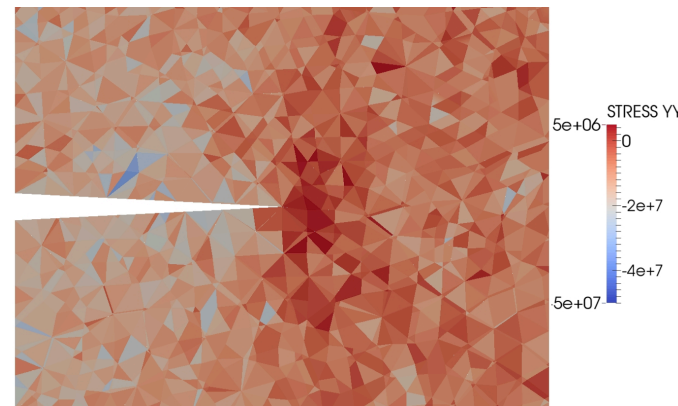
Solid concentration.



Adaptive mesh.

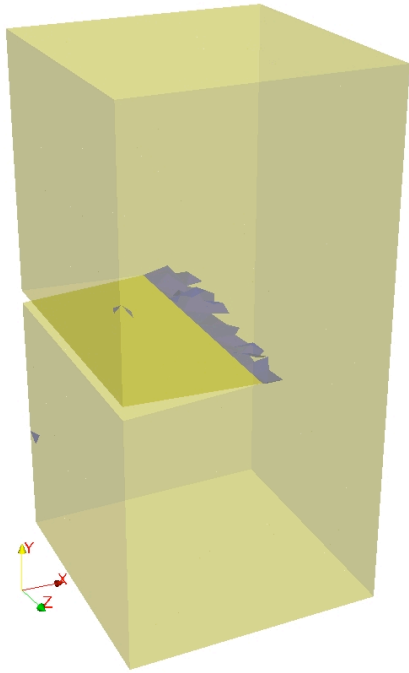


Two-dimensional fracture pattern.

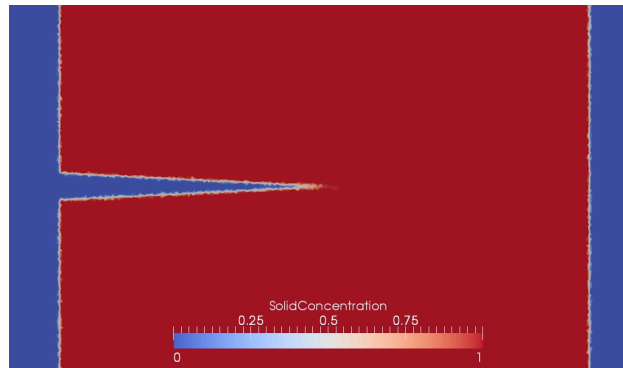


Vertical stress.

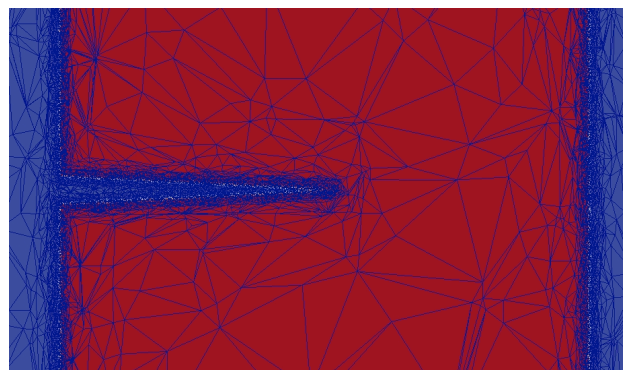
a. $t = 0.108$ ms.



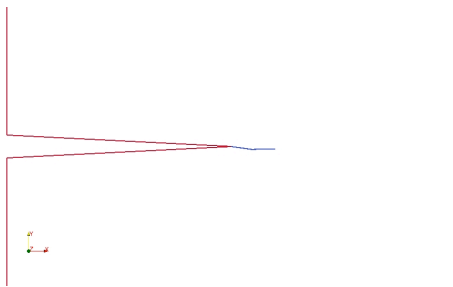
Three-dimensional fracture pattern.



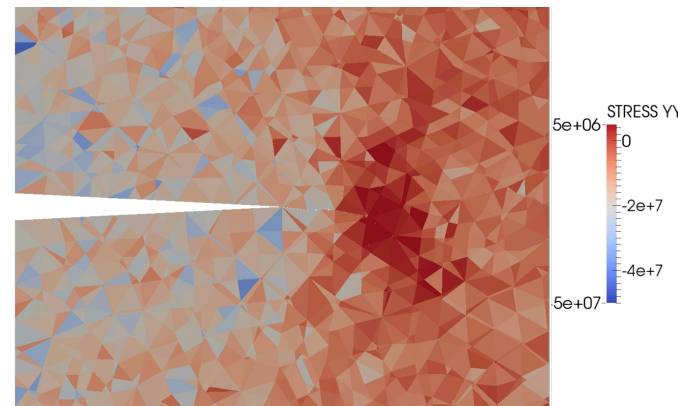
Solid concentration.



Adaptive mesh.

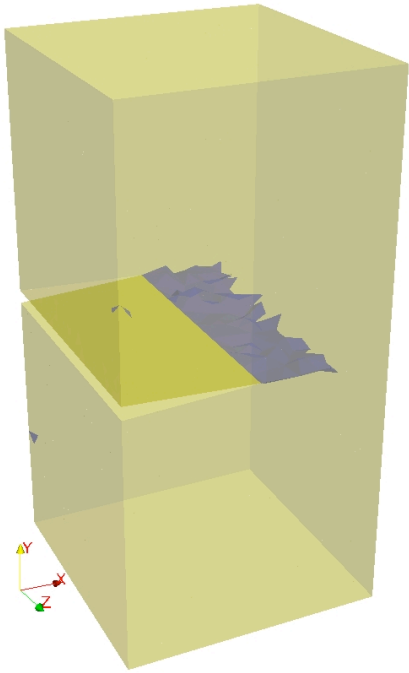


Two-dimensional fracture pattern.

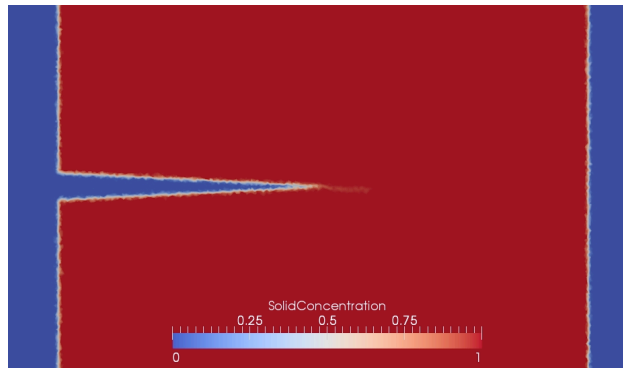


Vertical stress.

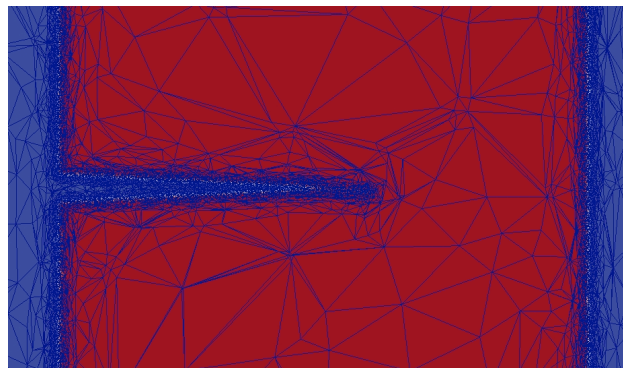
b. $t = 0.178$ ms.



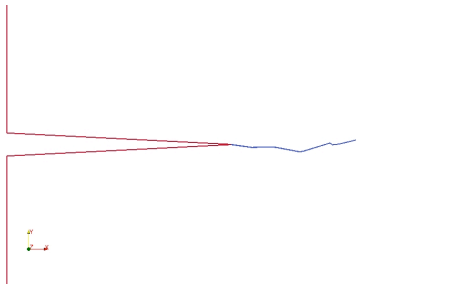
Three-dimensional fracture pattern.



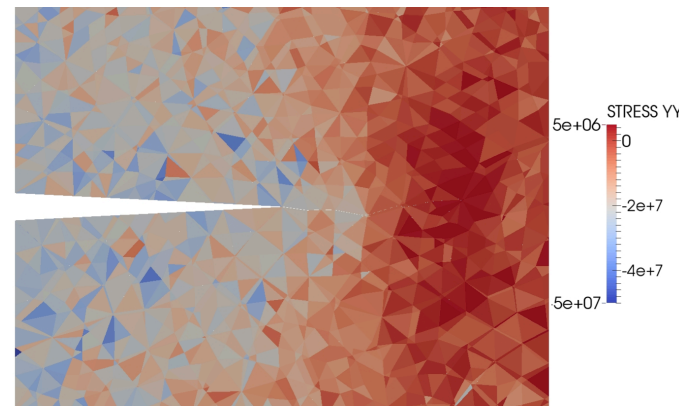
Solid concentration.



Adaptive mesh.

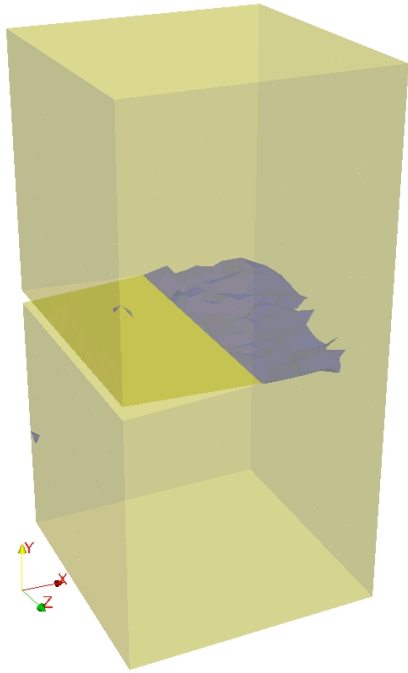


Two-dimensional fracture pattern.

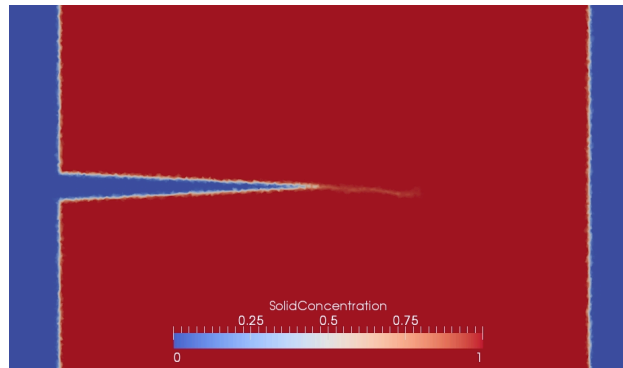


Vertical stress.

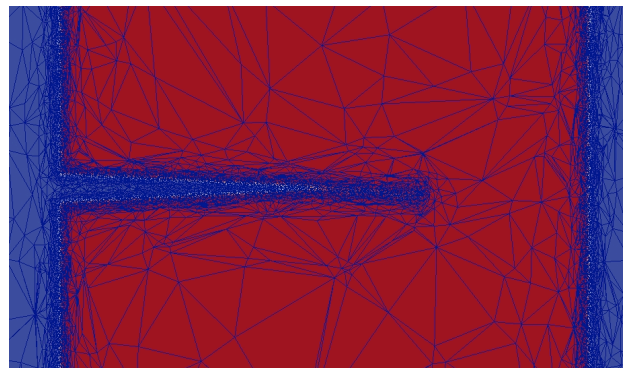
c. $t = 0.238$ ms.



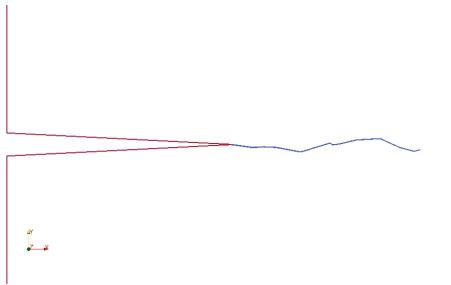
Three-dimensional fracture pattern.



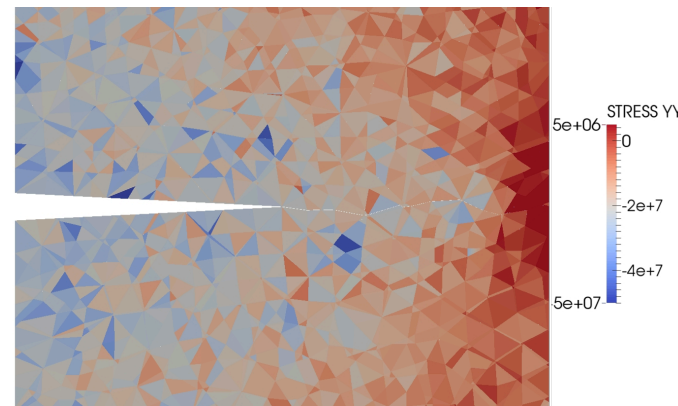
Solid concentration.



Adaptive mesh.

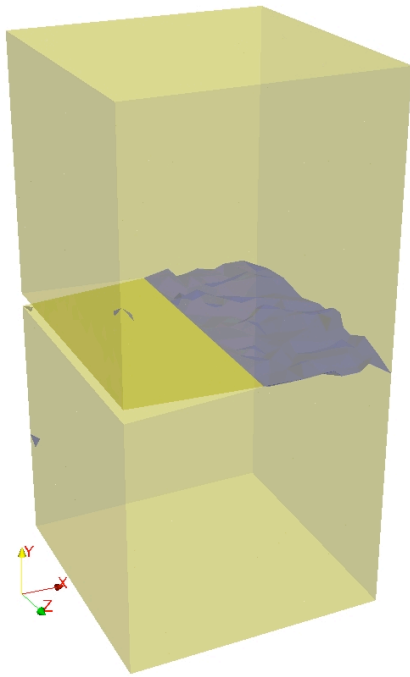


Two-dimensional fracture pattern.

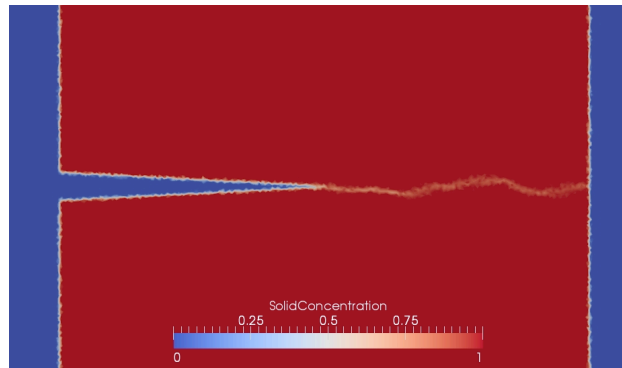


Vertical stress.

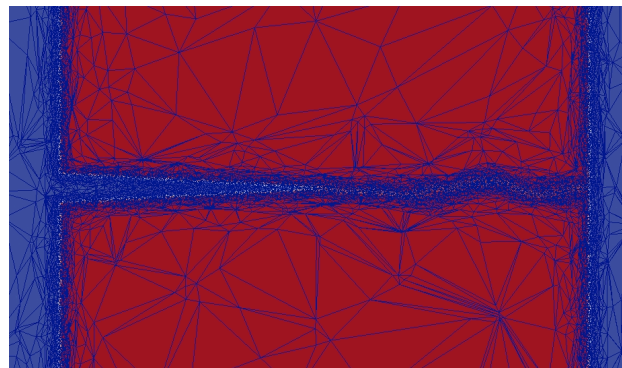
d. $t = 0.263$ ms.



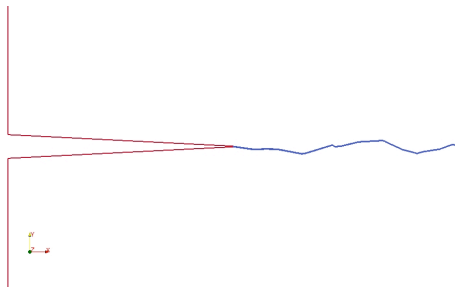
Three-dimensional fracture pattern.



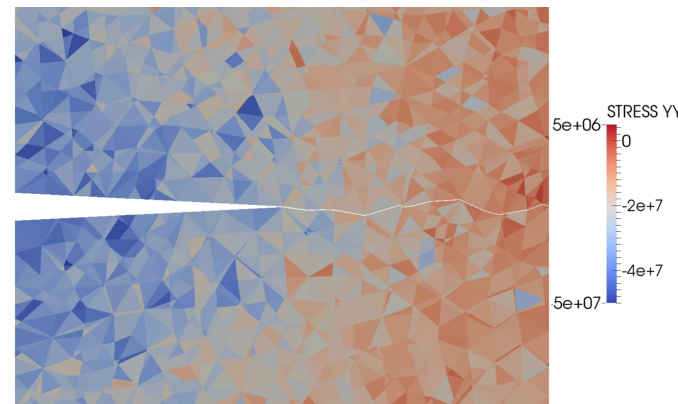
Solid concentration.



Adaptive mesh.



Two-dimensional fracture pattern.



Vertical stress.

e. $t = 0.378$ ms.

Fig. 7. Numerical results of the fluid-driven fracture simulation. *Three dimensional fracture pattern*: a semi-transparent colour scheme is adopted, where the yellow colour represents solid domain boundaries and pre-existing fracture surfaces, and the blue colour represents newly developed fracture surfaces. *Two-dimensional fracture pattern*: the local fracture development around the pre-existing fracture tip is shown in a cut plane as shown in Fig. 5b. *Solid concentration*: a parameter defined to distinguish the fluid domain and the solid domain, where the value of 1 means pure solids (red area) and 0 means pure fluids (blue area). *Adaptive mesh*: the adaptively updated mesh used by the fluid code is shown in the cut plane. Note that the intersection of three-dimensional meshes by cut planes tend to show what look like poor geometry triangular meshes but in fact the tetrahedral meshes themselves are of good qualities. *Vertical stress*: the contour of the vertical stress component (in the y -direction) σ_{yy} , where the red colour represents tension and the blue colour represents compression.

REFERENCES

1. Carter, B.J., J. Desroches, A.R. Ingraffea, and P.A. Wawrzynek. 2000. Simulating fully 3-D hydraulic fracturing. In *Modeling in Geomechanics*, ed. M. Zaman, G. Gioda, and J. Booker, 525-557.
2. Secchi, S. and B.A. Schrefler. 2012. A method for 3-D hydraulic fracturing simulation. *Int. J. Fracture*. 178: 245-258.
3. Munjiza, A. 2004. *The combined finite-discrete element method*. 1st ed. New York: Wiley and Sons.
4. Guo, L. 2014. *Development of a three-dimensional fracture model for the combined finite-discrete element method*. PhD thesis, Imperial College London.
5. Munjiza, A., K.R. Andrews, and J.K. White. 1999. Combined single and smeared crack model in combined finite-discrete element analysis. *Int. J. Numer. Meth. Eng.* 44: 41-57.
6. Guo, L., J.-P. Latham, and J. Xiang. 2015. Numerical simulation of breakages of concrete armour units using a three-dimensional fracture model in the context of the combined finite-discrete element method. *Comput. Struct.* 146: 117-142.
7. Viré, A., J. Xiang, F. Milthaler, P.E. Farrell, M.D. Piggott, J.-P. Latham, D. Pavlidis, and C.C. Pain. 2012. Modelling of fluid-solid interactions using an adaptive mesh fluid model coupled with a combined finite-discrete element model. *Ocean Dynam.* 62: 1487-1501.
8. Xiang, J., J.-P. Latham, A. Viré, E. Anastasaki, and C.C. Pain. 2012. Coupled Fluidity/Y3D technology and simulation tools for numerical breakwater modelling. In *Proceedings of the 33rd International Conference on Coastal Engineering, Santander, Spain*.
9. Lama, R.D. and V.S. Vutukuri. 1978. *Handbook on mechanical properties of rocks: testing techniques and results*. Trans Tech Publications.
10. Nolte, K.G. 1988. Fluid flow considerations in hydraulic fracturing. In *SPE Eastern Regional Meeting, SPE-18537, Charleston, USA*.
11. Monteagudo, J.E.P., A.A. Rodriguez, and H. Florez. 2011. Simulation of flow in discrete deformable fractured porous media. In *SPE Reservoir Simulation Symposium, SPE 141267, The Woodlands, USA*.
12. Carrier, B. and S. Granet. 2012. Numerical modelling of hydraulic fracture problem in permeable medium using cohesive zone model. *Eng. Fract. Mech.* 79: 312-328.